Special Issue on COVID-19 Aerosol Drivers, Impacts and Mitigation (III)

Aerosol and Air Quality Research, 20: 1530–1540, 2020
Publisher: Taiwan Association for Aerosol Research
ISSN: 1680-8584 print / 2071-1409 online
https://doi.org/10.4209/aaqr.2020.05.0226

Impact Assessment of COVID-19 on Variations of SO_2, NO_2, CO and AOD over East China

Mikalai Filonchyk[1,2*], Volha Hurynovich[1,2], Haowen Yan[1,2*], Andrei Gusev[3], Natallia Shpilevskaya[3]

[1] *Faculty of Geomatics, Lanzhou Jiaotong University, Lanzhou 730070, China*
[2] *Gansu Provincial Engineering Laboratory for National Geographic State Monitoring, Lanzhou 730070, China*
[3] *Francisk Skorina Gomel State University, Gomel 246019, Republic of Belarus*

ABSTRACT

The COVID-19 (Coronavirus Disease 2019) broke out in the late of 2019. On January 23 in Wuhan, and later in all other cities of the country, there were taken measures to control the spread of the virus through quarantine measures. This article focused on East China and attempted to assess comprehensively the environmental impact of the COVID-19 outbreak. This study analyzed satellite observational data of sulfur dioxide (SO_2), nitrogen dioxide (NO_2), carbon monoxide (CO) and aerosol optical depth (AOD) in the period before the outbreak of the epidemic and during the implementation of preventive measures and control of COVID-19, as well as compared it with the data obtained in the same period of 2019. The results of the analysis showed that the COVID-19 lockdown improved air quality in the short term, but as soon as coal consumption at power plants and refineries returned to normal levels due to the resumption of their work, pollution levels returned to their previous level. The levels of CO and NO_2 showed the most significant decrease (20 and 30%), since they were mainly associated with a decrease in economic growth and transport restrictions that led to a change in energy consumption and a reduction in emissions. This study can complement the scientific community and environmental protection policy makers, not only to assess the impact of outbreak on air quality, but also for its effectiveness as a simple alternative program of action to improve air quality.

Keywords: COVID-19; East China; Air pollution; Remote sensing; Anthropogenic activities.

INTRODUCTION

On December 31, 2019, Chinese authorities informed the World Health Organization (WHO) of an outbreak of unknown pneumonia. From January 23, the city of Wuhan was quarantined, and from January 24, restrictive measures to prevent the spread of infection began to be introduced in many cities of the country. Transport links with a number of megacities were limited, quarantining 60 million people in 17 cities of Hubei Province. There were recorded cases in each unit at the provincial level in China, a few weeks later, the virus globally spread first to other Asian countries, and later to North America, Europe and other countries. World Health Organization announced pandemic of this disease on March 11.

It turned out that the new type of coronavirus was almost 70% identical to the SARS-CoV (Severe Acute Respiratory Syndrome Coronavirus) (Hui *et al.*, 2020). The new coronavirus was first assigned with the code 2019-nCoV, and from February 11 it was renamed SARS-CoV-2 (WHO 2020a). The infectious disease that it caused was called COVID-19 (Coronavirus Disease 2019). A hallmark of the current pandemic that makes it difficult to struggle, it is its long incubation period, which is usually about 5 days, but can last from 2 to 14 days (CDC, 2020; Holshue *et al.*, 2020). In severe cases of the course of the disease, COVID-19 can cause pneumonia, acute respiratory syndrome, kidney failure, and even death (Perlman, 2020). So on June 5, 2020, the total of COVID-19 cases surpassed 6.5 million and over 387,298 deaths worldwide (WHO, 2020b).

As countries became locked, industrial activity ceased throughout the world. Among many other sectors of the economy, transport was the most affected sector due to lockdown. Road and air transport had been stopped, as many governments had severely restricted the movement of people (Muhammad *et al.*, 2020). In addition, the pandemic had affected not only the transport sector, but also the industrial and manufacturing sectors. Global oil demand has

* Corresponding author.
E-mail address: haowen2010@gmail.com (H. Yan); filonchyk.mikalai@gmail.com (M. Filonchyk)

plummeted and prices plummeted as industry and transport sectors around the world have stopped. The global outbreak and spread of COVID-19 not only seriously threatened public health, but also seriously prevented global economic growth (Wang *et al.*, 2020; Wu *et al.*, 2020).

This analysis of early data suggested that government policies that directly reduced human activity, commercial demand, and transport could effectively and quickly reduce urban air pollution (Filonchyk and Hurynovich, 2020a; Jribi *et al.*, 2020; Xu *et al.*, 2020a; Zhu *et al.*, 2020). That is, environmental pollution would increase with economic growth. In general, the significance and consequences of a lockdown were still poorly understood and studied, and could probably play an important role in restoring air quality. The nationwide lockdown during the time of COVID-19 pandemic provided a unique opportunity to work in this direction. Therefore, a quantitative assessment of air pollution was necessary in order to ultimately take measures to limit air quality, especially when such alternative control measures were necessary. This study is an attempt to evaluate the usefulness of locking as an alternative strategy to reduce air pollution in East China. The main objectives of this study are: to compare the concentrations of atmospheric pollutants (sulfur dioxide (SO_2), nitrogen dioxide (NO_2) and carbon monoxide (CO)) and aerosol properties (aerosol optical depth (AOD)) in the period before the lockdown and during the implementation of preventive control measures COVID-19. By focusing on East China, this study is expected to be a real complement to the scientific community and environmental protection policy makers, not only to assess the impact of lockdown on air quality, but also for its effectiveness as a simple alternative program of action to improve air quality.

DATA AND METHODS

Sulfur Dioxide (SO_2) and Nitrogen Dioxide (NO_2) Data

Sulfur dioxide (SO_2) and nitrogen dioxide (NO_2) emission data obtained from Ozone Monitoring Instrument (OMI) on board the AURA satellite launched in 2004 as part of the NASA EOS (Earth Observation System) were used, which performed measurements of solar radiation reflected by the atmosphere and the Earth's surface in the range from 270 to 500 nm and with a spectral resolution of 0.5 nm. The width of the recorded strip of the surface, which is about 2600 km, and the satellite's orbital period of 98.8 minutes, make it possible to carry out measurements on a global scale and cover almost the entire Earth's surface in a day. In the OMI mode, designed for shooting on a global scale, the pixel size when shooting in the nadir direction is 13 × 24 km along and across the shooting strip, respectively (Levelt *et al.*, 2006). The spectrometer measurement data were used to determine the vertical profiles of ozone, the concentrations of atmospheric gases such as NO_2, SO_2, HCHO, BrO and OClO, the surface illuminance, as well as a number of characteristics of aerosol and clouds. The data processing algorithm provided information on elevated SO_2 concentrations at three altitudes: 2 km (anthropogenic SO_2), 5 km (passive volcanic degassing) and 15 km (large explosive eruptions) (Krotkov *et al.*, 2006). The method was based on measuring the spectral characteristics of sunlight scattered in the atmosphere and reflected from the surface of the Earth. Comparison of the initial and reflected spectra provided information on the distribution and concentration of trace elements, O_3 and SO_2, as these gases absorb and scatter part of the incoming sunlight. The units of SO_2 concentration were Dobson Units (DU) (1 DU = 2.69×10^{16} molecules cm^{-2}). To ensure data quality, SO_2 data were excluded from observations with a cloud radiance fraction of greater than 0.2 and solar zenith angle > 70° (Krotkov *et al.*, 2016). It is worth noting that negative SO_2 values in this article could be caused by interference between the SO_2 and O_3 absorption and could usually indicate very low SO_2 values (Yan *et al.*, 2012). This is because in the UV region SO_2 and O_3 have strong absorption and can interfere with each other during measurement. This is particularly affected by O_3 interference in measuring SO_2, which can show a concentration of SO_2 less than the actual value, which can lead to serious measurement errors. When the O_3 concentration is the main ruler of the mixing ratio of SO_2 and O_3, the result of SO_2 is minus.

As for NO_2, the OMI instrument allowed to determine the total NO_2 content in the vertical column of the atmosphere as the total number of NO_2 molecules between the Earth's surface and the tropopause per unit area (Boersma *et al.*, 2004). Search errors in remote unpolluted areas were due to uncertainties in spectral fitting and (0.7×10^{15} molecules cm^{-2}) (Boersma *et al.*, 2007). NO_2 content in the vertical column of the atmosphere was calculated by dividing the inclined content by the air mass value of NO_2, which depended on a number of parameters, including the geometry of the observations, the surface albedo, the shape of the vertical profile of NO_2 and cloud characteristics (height, density, and sky coverage) (Boersma *et al.*, 2004). NO_2 data was provided only if the cloud radiance fraction did not exceed 0.3 (i.e., close to clear sky) and solar zenith angle > 85° to ensure data quality. In this study, we used daily Level 3 Aura/OMI SO_2 and NO_2 data products with a spatial resolution of 0.25 × 0.25° to study SO_2 and NO_2 emission in the Hubei Province. OMI Level 3 SO_2 and NO_2 data from NASA GES DISC archive.

Carbon Monoxide (CO) Data

Atmospheric Infrared Sounder (AIRS) introduces the grating spectrometer aboard AQUA satellite, launched on May 4, 2002. The device was designed to support climate research and improve weather forecasting, and to display the concentration of a number of gases in the atmosphere, including water vapor, carbon dioxide, carbon monoxide, ozone and methane. The main instrument of the complex is the AIRS infrared spectrometer, which has 2378 spectral channels and is capable of recording the intensity of outgoing thermal radiation in the ranges 3.74–4.61 μm (2169–2674 cm^{-1}), 6.20–8.22 μm (1217–1613 cm^{-1}), 8.8–15.4 μm (649–1136 cm^{-1}) with high spectral resolution ($\lambda/\Delta\lambda$) ~1200 and a 13.5 km footprint at nadir (Aumann *et al.*, 2003; Pagano *et al.*, 2003; 2011). These spectral ranges include the absorption zones of carbon dioxide (4.3 and 15 μm), water vapor (6.3 μm), methane (7.6 μm) and ozone (9.6 μm) important for reconstructing atmospheric parameters (Chahine *et al.*, 2005). The most efficient CO extraction

process in the middle AIRS troposphere is from 300 to 500 hPa (9–5.5 km); therefore, data from a height of 400 hPa (7 km) will be used in this work, and CO data will be extracted globally in day and nighttime under clear and cloudy sky conditions (Warner *et al.*, 2007; Xiong *et al.*, 2008). In this article, we used the data of Level 3v6 (spatial resolution 1 × 1°) only daily measurements of CO of the ascending orbit (ascending, i.e. around 12:30–13:30 local solar time (LST)). AIRS CO products were obtained from Goddard Earth Sciences Data and Information Services Center (GES/DISC).

Aerosol Optical Depth (AOD) Data

As a component of the NASA EOS, Moderate Resolution Imaging Sectroradiometer (MODIS) on TERRA and AQUA satellites provides level 2 aerosol products. Due to the fact that the AQUA satellite crossing the equator close to the AURA satellite crossing time, it was decided to use aerosol optical depth (AOD) data obtained by the MODIS-AQUA satellite with a spatial resolution of 10 km and with the quality flag of at least 2 (QA = 2 and 3). Based on previous studies, the MODIS seasonal observation cycle is reported to be consistent with ground based observations, including the Aerosol Robotic Network (AERONET) sun and sky radiance measurements (Kim *et al.*, 2007). Therefore, AOD data can be considered suitable as an assessment tool for studying spatio-temporal changes in aerosol and can be used for cross-comparison with measured gaseous pollutants. The uncertainty of MODIS AOD is $\pm 0.05 \pm 0.20 \times AOD_{AERONET}$ (Sayer *et al.*, 2013) and $\pm 0.05 \pm 0.15 \times AOD_{AERONET}$ (Levy *et al.* 2013) over the land. MODIS AOD data was obtained from NASA's Level-1 and Atmosphere Archive and Distribution System (LAADS) Distributed Active Archive Center (DAAC).

RESULTS AND DISCUSSION

Changes in Economic Activity and Energy Consumption

From the end of 2019 to the present, the COVID-19 epidemic had spread around the world, exacerbating the epidemiological situation and leading to serious consequences for human health (Xu *et al.*, 2020a, 2020b). To eliminate the spread of the epidemic, the Chinese government decided to implement immediately measures to control and prevent the spread of the virus. Since January 23, the city of Wuhan has been quarantined, and since January 24 other cities of the province, approximately 60 million people have been influenced by the restrictions. Air and rail traffic between cities were banned, and road links were closed. Later, various kinds of preventive measures were taken in all regions of the country. At many enterprises in the country production was suspended. In order to suppress epidemic throughout the country, restriction of population movement has been adopted, with most of the country's population facing various forms of movement restrictions (Griffiths and Woodyatt, 2020). In many urban residential complexes, fences and gratings were installed to block all entrances and exits. The exit was through the only gate where the guards were on duty around the clock. In a number of cities, the creation of entire networks of controlling and patrolling areas was initiated to identify quickly and isolate patients with suspected cases of infection with COVID-19, as well as those who came into contact with them. Restriction measures included driving restrictions on all non-emergency vehicles. The introduction of strict measures to curb the spread of the COVID-19 (forced self-isolation, quarantine, closing borders and production, limiting air traffic) could have not only a positive impact on the environment, but also led to a decrease in economic growth. The outbreak of COVID-19 had some negative effects on the economy (Xu *et al.*, 2020b, Zhao *et al.*, 2020). Therefore, the above preventive and control measures could be closely related to air quality.

China's energy consumption had dropped significantly due to a significant reduction in urban transport and industrial activity during the quarantine period. China is the world leader in coal consumption, and coal resource dominates energy consumption (BP, 2019). Myllyvirta (2020) reported a decline in coal consumption in the country during the lockdown period. Every winter, during the Lunar New Year period, the whole country suspends activity for a week, that is why most of the industries stop working. The holiday has a significant short-term reduction in energy consumption (Myllyvirta, 2020). The resumption of production, which begins after the Spring Festival, leads to an increase in energy consumption, but 2020 was an exception due to the outbreak of COVID-19. There was a decrease in coal consumption for industrial purposes compared to 2019. This was because the epidemiological situation led to that the country's government decided to extend the New Year holidays in order to prevent the spread of the virus (Wang and Su, 2020). By mid-March, according to the Ministry of Industry and Information Technology (MIIT), state and large industrial companies resumed their work by 90%; since March 24, the Chinese authorities removed most of the previously imposed social and economic restrictions, stating that the spread of the virus in this the country is "mostly blocked."

Spatial Distribution of Air Pollutants

Air pollution is one of the main environmental health problems that affects everyone in low, middle and high income regions. Air pollution is one of the main environmental health risks. The lower the levels of air pollution shows better health of the population with the cardiovascular and respiratory, both in the long and short term. Therefore, it is very important to monitor constantly air quality in order to assess the impact of pollutants on human health.

This study will focus on East China (denoted by the black box, latitude: 28–42°N, longitude: 108–124°E). The satellite-derived mean columns of AOD, SO_2, NO_2 and CO in January, February and March 2019 and 2020 are shown in Figs. 1–4 (white color indicates the absence of AOD data). High concentrations of pollutants have been reported mainly over eastern China. In addition, it is worth noting the Pearl River Delta and Sichuan Basin, which are also subject to high concentrations of pollutants, although significantly lower than in East China.

Fig. 1 shows the average spatial distribution of MODIS AOD for the first quarter (including January, February, and March) of 2019 and 2020. One of the possible causes of

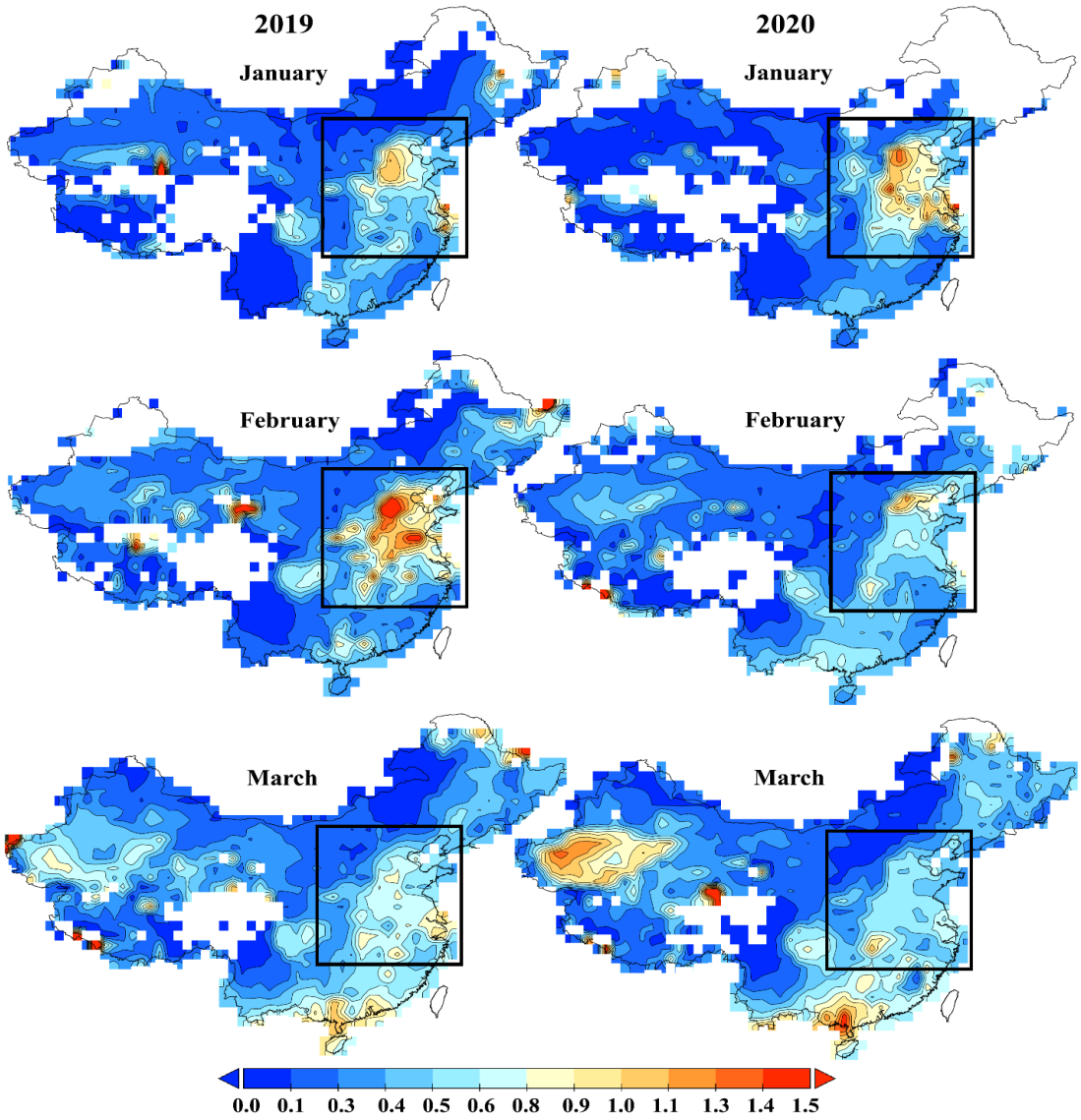

Fig. 1. Spatial distribution of AOD at 550 nm from MODIS.

pollution is a high degree of urbanization, a high population density and a large number of mobile sources (for example, vehicles), emissions from which lead to high aerosol loads. Also possible sources of aerosols can be associated with the burning of fossil fuels (oil and coal) at power plants and in industry, the burning of coal and the burning of biomass for domestic heating, as well as the transfer of dust over long distances. High AOD were observed at North China Plain (above 0.8) and Yangtze River Delta (above 0.7), which is associated with high emissions from factories and the country's largest coal-fired power stations (Beilun, Waigaoqiao, Jiaxin, Ninghai, Yangcheng and Zouxian Power Stations). It is worth noting that China consumed 641.2 million tonnes of oil, which accounted for 13.8% of global oil consumption; 243.3 million tons of oil equivalent (MTOE) of natural gas, which accounted for 7.4% of global natural gas consumption; and 1906.7 MTOE of coal, which accounted for 50.5% of global coal consumption (BP, 2019). In addition, high coastal AOD can be the result of strong emissions from ships, as well as long-range aerosol transport from North China Plain and strong hygroscopic growth of aerosol due to high relative humidity, especially in the south region (Huang *et al.*, 2018; Ahmed *et al.*, 2020). AOD levels over East China were much higher than in other regions of the country.

Figs. 2 and 3 showed the spatial distribution of SO_2 and NO_2 over the study period. Sulfur dioxide (SO_2) was produced by burning fossil fuels (coal and oil) and smelting mineral ores containing sulfur, as well as various chemical processes. The main anthropogenic source of SO_2 was the burning of sulfur-containing fossil fuels for heating homes, generating electricity, refining, and from cars (Filonchyk *et al.*, 2020b). Since SO_2 was mainly produced by burning coal, the highest SO_2 values were recorded in North China Plain (above 0.45 DU), where there are power plants and coal mining industries (Fig. 2) (Krotkov *et al.*, 2016). The SO_2 values over the Yangtze River Delta (above 0.43 DU) were similar to North China Plain, mainly because there are a large number of vehicles in the Yangtze River Delta region.

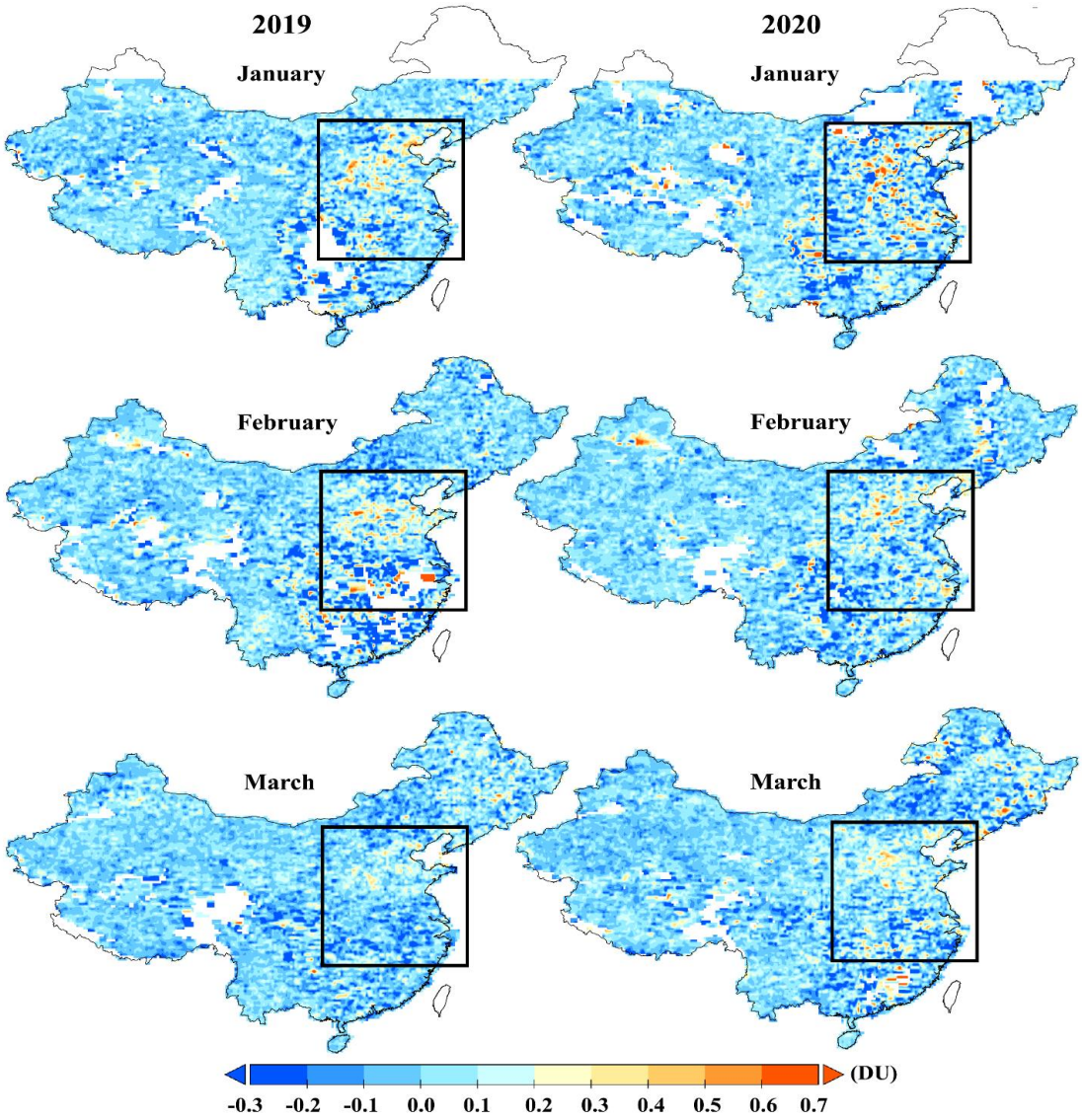

Fig. 2. Spatial distribution of planetary boundary layer (PBL) SO_2 from OMI.

Thus, high concentrations of SO_2 were found in highly industrialized regions of the country, such as the North China Plain (Beijing-Tianjin-Hebei region) and Yangtze River Delta, as well as in other coastal regions of the country (Fig. 2). As for NO_2 (Fig. 3), the main sources were combustion processes (heating, power generation, engine operation of cars and ships), high NO_2 concentrations were similar to SO_2, which are located in highly urbanized areas such as Beijing, Tianjin, Hangzhou, Shanghai, Shijiazhuang, Nanjing. Due to its high solubility, the presence of SO_2 and NO_2 in the lower atmosphere was not large, depending on the season and terrain, it can be up to 2 days (Renuka *et al.*, 2020). This interval is too short for these air pollutants to spread globally. Therefore, in neighboring geographical areas, where both large and moderate emissions of SO_2 and NO_2 were carried out, a large difference in the concentrations of SO_2 and NO_2 could be observed in the atmosphere. It can be concluded that SO_2 and NO_2 arise primarily in highly developed industrial regions, and also short distance transportation from these regions with heavier pollutants to neighboring regions is possible. Unlike to AOD, SO_2 and NO_2 showed the highest levels in the first two months of the year (January and February). The high level of SO_2 during this period may be associated with additional emissions from house heating and may decrease during the warmer period, due to the absence of the need for heating the room. With an increase in precipitation, SO_2 easily dissolves in water, form acidic gases can be carried by powerful air currents for hundreds of kilometers (Hu *et al.*, 2018). High AOD values (above 0.6) were observed in approximately the same areas where NO_2 had high values, but because of the much longer residence time of aerosol particles in the atmosphere, in contrast to several hours for NO_2 and SO_2, they can be transported over long distances. High AOD values were also observed in the Pearl River Delta and Sichuan Basin.

As known, the main anthropogenic sources of CO in the atmosphere are motor vehicles, power plants and industrial emissions. Satellite data showed a similar spatial distribution of

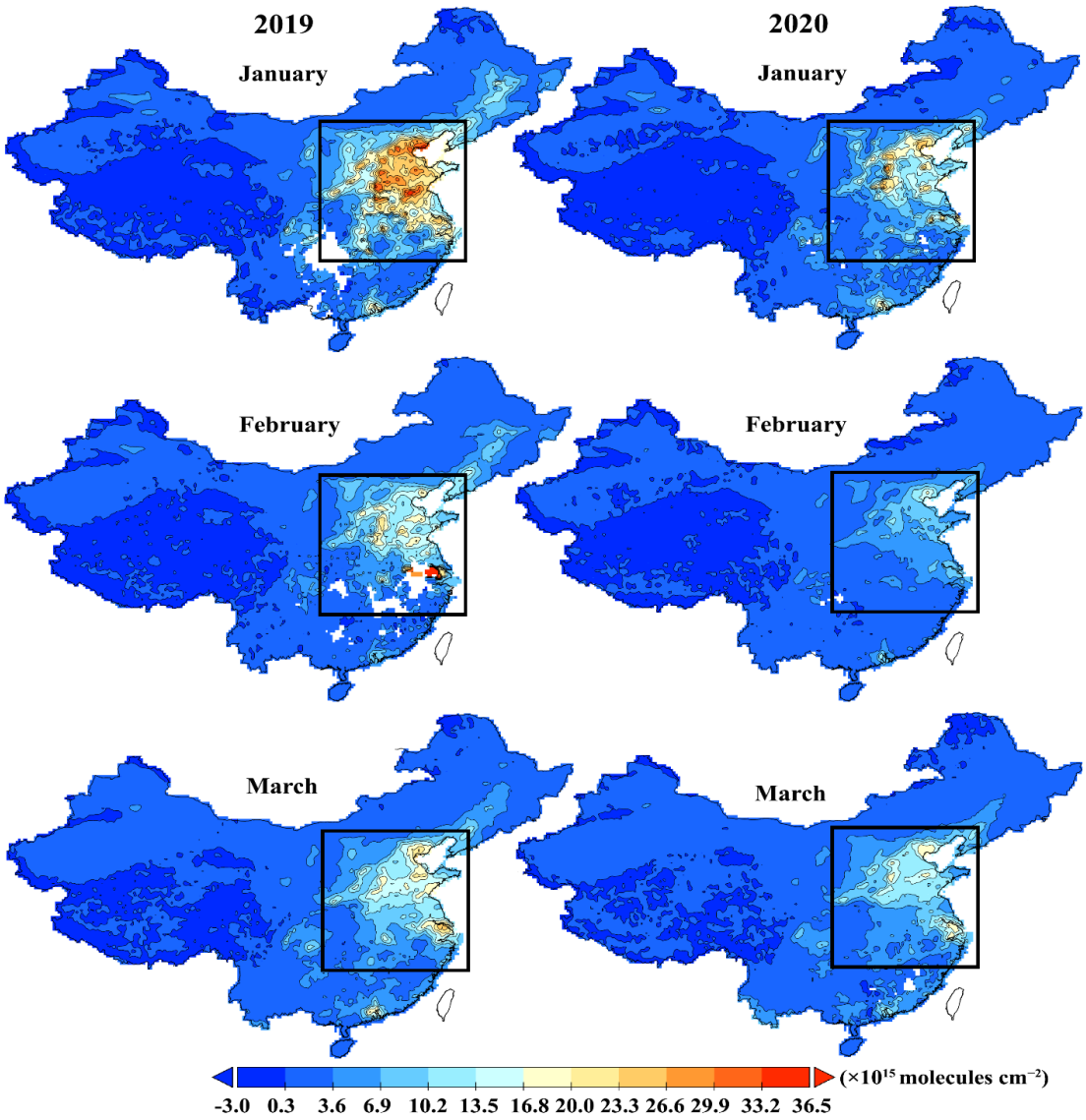

Fig. 3. Spatial distribution of tropospheric NO_2 from OMI.

CO concentration with other pollutants. Areas with a high concentration of CO were concentrated almost over the entire territory of East China (Fig. 4), and focus can be also noticed above the Pearl River Delta and Sichuan Basin, as well as in the south of the country. This distribution is also similar to previous studies (Liu *et al.*, 2011; Kang *et al.*, 2019). The concentration distribution in the CO column was closely related to population density and locality. Emissions from anthropogenic activities have a significant impact on the concentration of CO. It had been proven that areas with low CO concentrations were often associated with the topography and altitude. Low concentrations of CO were often located in the high elevation region due to the low mass of atmospheric column and low anthropogenic activity (Zhang *et al.*, 2016). Although against the background of East China, the level of CO pollution in the troposphere of other regions of the country did not look so dramatic (taking into account population density, the scale of industrial production, geographical, topographic and climatic features and other factors), CO could be relatively high due to its relatively more long term in the atmosphere. Therefore, the spatial distribution of CO was more uniform throughout the study region.

Temporal Variations of Pollutants

MODIS and AIRS instrument on the AQUA satellite and OMI on the AURA satellite collect data on AOD, CO and SO_2 and NO_2 in the troposphere of East China. Figs. 1–4 showed spatial distributions, and Fig. 5 showed the temporal distributions of aerosols and pollutants in the first quarter (January, February and March) of 2019 and 2020. Taking into account the fact that, since January 23, quarantine measures were taken first in Wuhan, and later throughout China, this date was a dividing line between the period before and after the introduction of quarantine measures. In general, AOD, SO_2, NO_2 and CO both in East China and in the whole country were significantly lower in February than in the previous period of 2019.

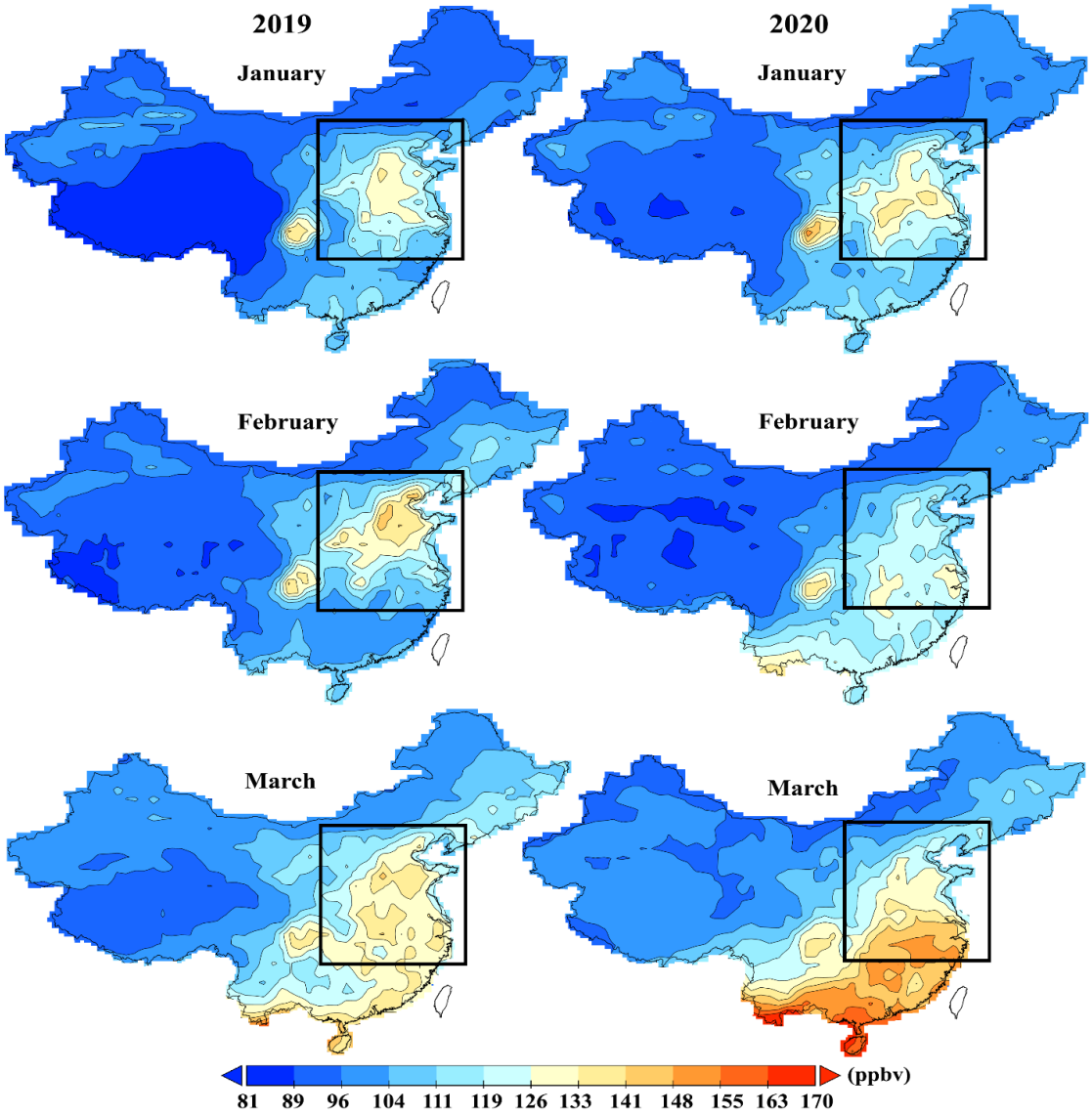

Fig. 4. Spatial distribution of CO at 400 hPa from AIRS.

In the first three months of 2020, the concentration of pollutants showed a significant decline compared to the same period in 2019 (Figs. 1–5). The levels of air pollutants were high about a week (January 15) before the Chinese government introduced strict prevention and control actions throughout the country (Fig. 5). Due to the fact that East China is one of the main industrial regions of the country, due to intensive industrial activity, a huge amount of SO_2, NO_2, CO and other aerosols were released into the atmosphere. However, after the country adopted strict restrictive measures to control COVID-19, which led to the suspension of many plants and enterprises, emissions of SO_2, NO_2 and CO throughout the country were significantly reduced, leading to improved air quality. Another reason for the reduction in emissions may be due to the Lunar New Year holiday (from February 5 to 20 in 2019 and from January 24 to February 8 in 2020), which was consistent with the results of previous studies (Lai and Brimblecombe, 2017; Zhang *et al.*, 2017; Safarian *et al.*, 2020). The reduced use of coal and crude oil led to a reduction in CO emissions of about 20% compared to the same two-week period after the Lunar New Year in 2019. It is worth noting that as soon as industrial production began to resume (the second half of February), the amount of emissions began to increase, this was especially evident in CO.

There was made a comparison of the values of SO_2, NO_2, CO, and AOD in the first three months of 2020 with the same values in the period of 2019. The results showed that emissions of pollutants in East China were lower than in the same period in 2019. Although, in March 2020, CO concentrations in the southern regions of the country were higher than 2019 (Fig. 4). This was due to emissions outside the country, namely in Vietnam, where the prevention and control measures for the spread of COVID-19 were not so strict, therefore, the CO cloud stretched in a continuous strip from the northern borders of Vietnam, the Pearl River Delta and further north to the Yangtze River Delta, covering most of the territory.

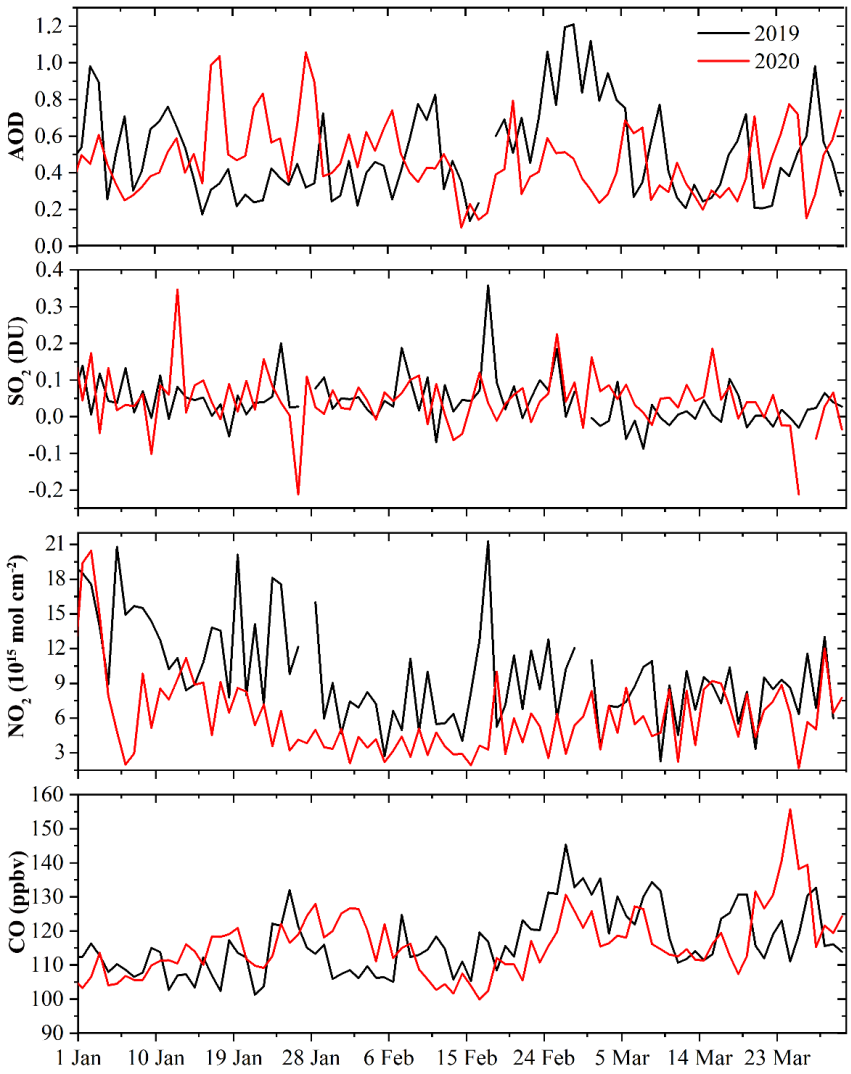

Fig. 5. Temporal variability of AOD, SO_2, NO_2 and CO over East China.

Air pollution, which is closely associated with the burning of fossil fuels, is another confirmation of the reduction in the use of fossil fuels in satellite NO_2 measurements. In the two-week period after Lunar New Year 2020, average levels were reduced by about 30%, compared with the same period in 2019, as shown in Fig. 5. China's energy consumption is dominated by energy-intensive industries and freight transportation, with residential electricity consumption and in commercial premises, private cars play a relatively minor role (Zhang *et al.*, 2015; Filonchyk *et al.*, 2020b). As can be seen from Fig. 5, the AOD values in 2020 were relatively high, and this period, when there were restrictions on movement and more cars were off, and most enterprises were closed. This may be due to blast furnaces, which continued to operate for extended periods, while most power plants shut down, at best, only part of their boilers.

In order to prevent the spread of COVID-19 throughout the country, local authorities have taken restrictive measures like closed administration and travel restrictions. Fig. 2 showed the concentration of SO_2 in the atmosphere for three months in 2019 and 2020. Compared to 2019, in 2020 SO_2 emissions decreased slightly. The restrictions that China had taken to combat COVID-19 had not only slowed domestic economic growth, but had actually reduced air pollutant emissions. However, it is worth assuming that these reductions were short-term, and in the long term, a recovery to previous years is inevitable. Therefore, it is necessary to take into account measures to protect the environment during economic recovery.

In general, studies conducted in other regions during the lockdown period also indicate a decrease in the concentration of pollutants. Thus, a sharp decrease in the concentration of $PM_{2.5}$ (up to –29.8%), PM_{10} (up to –22.8%), SO_2 (up to –18.1%), NO_2 (up to –54.3%) and CO (up to –64.8 %) was observed in urban areas of São Paulo, Brazil, during lockdown (March 24–April 20, 2020) compared to the same period of 2015-2019 (Nakada *et al.*, 2020). In Almaty, Kazakhstan, $PM_{2.5}$ concentrations during the lockdown period (March 19 to April 14, 2020) were reduced by 21% compared to the same period in 2018–2019 (Kerimray *et al.*, 2020). A study in three cities of Hubei Province (Wuhan, Jingmen, and Enshi) showed that in these cities in February 2020,

when measures were taken to prevent and control epidemics, the mass concentrations of $PM_{2.5}$, PM_{10}, NO_2, SO_2 and CO were 30.1%, 40.5%, 61.4%, 33.4% and 27.9%, and lower than in the same period of 2017–2019 (Xu *et al.*, 2020a).

Coal consumption at power plants and refineries returned to normal levels by the end of March. SO_2, NO_2, CO, and AOD pollution levels measured from both NASA satellites and national air quality monitoring stations (Xu *et al.*, 2020a) have also returned to normal, indicating that current levels of emissions in both urban areas, in industrial centers, too, they were close to pre-crisis levels (Myllyvirta, 2020; Xu *et al.*, 2020b).

CONCLUSIONS

The Lunar New Year holiday (from January 24 to February 8 in 2020) and the COVID-19 epidemic prevention and control measures in February and March 2020 had a significant impact on air quality not only in East China, but throughout country. After the country adopted strict restrictive measures to control COVID-19, which led to the suspension of many plants and enterprises, emissions of SO_2, NO_2 and CO across the country were significantly reduced, leading to improve air quality. This implies a close relationship between economics and environmental pollution. The decrease in economic activity and transport restrictions directly affected the change in energy consumption in the country and effectively reduced environmental pollution. Coal consumption at power plants and refineries returned to normal levels by the end of March. Pollution levels of SO_2, NO_2, CO, and AOD measured from NASA satellites returned to normal by the end of March. This indicated that the intensity of anthropogenic activity in the region had returned to the level of past years. The reduced use of coal and oil led to a reduction in CO emissions of about 20% and NO_2 by 30% in comparison to the same period after Lunar New Year in 2019. High AOD values may be associated with blast furnaces, which continued to operate for extended periods, while most power plants were shut down, at best, only part of their boilers. Although COVID-19 had a significant negative impact on economic activity and transport, on the other hand it showed lightened pressure on the environment.

DECLARATION OF CONFLICTS OF INTEREST

The authors declared that they have no conflict of interests.

ACKNOWLEDGEMENTS

The work was financially supported by the National Key R&D Program of China (2017YFB0504203), the China Postdoctoral Science Foundation Funded Project (2018M633605), the Postdoctoral Fund of Lanzhou Jiaotong University (2018BH03001).

REFERENCES

Ahmed, A., Nawaz, R., Woulds, C. and Drake, F. (2020). Influence of hydro-climatic factors on future coastal land susceptibility to erosion in Bangladesh: A geospatial modelling approach. *J. Geovis. Spat. Anal.* 4: 6. https://doi.org/10.1007/s41651-020-00050-x

Aumann, H.H., Chahine, M.T., Gautier, C., Goldberg, M.D., Kalnay, E., McMillin, L.M. and Strow, L.L. (2003). AIRS/AMSU/HSB on the Aqua mission: Design, science objectives, data products, and processing systems. *IEEE Trans. Geosci. Remote Sens.* 41: 253–264. https://doi.org/10.1109/TGRS.2002.808356

Boersma, K.F., Eskes, H.J. and Brinksma, E.J. (2004). Error analysis for tropospheric NO_2 retrieval from space. *J. Geophys. Res.* 109: D04311 https://doi.org/10.1029/2003JD003962

Boersma, K.F., Eskes, H.J., Veefkind, J.P., Brinksma, E.J., van der A, R.J., Sneep, M., van den Oord, G.H.J., Levelt, P.F., Stammes, P. and Gleason, J.F. (2007). Near-real time retrieval of tropospheric NO_2 from OMI. *Atmos. Chem. Phys.* 7: 2103–2118. https://doi.org/10.5194/acp-7-2103-2007

BP (2019). BP statistical review of world energy 2019, 68th edition. https://www.bp.com/content/dam/bp/business-sites/en/global/corporate/pdfs/energy-economics/statistical-review/bp-stats-review-2019-full-report.pdf

Centers for Disease Control and Prevention (CDC) (2020). https://www.cdc.gov/coronavirus/2019-ncov/symptoms-testing/symptoms.html?CDC_AA_refVal=https%3A%2F%2Fwww.cdc.gov%2Fcoronavirus%2F2019-ncov%2Fabout%2Fsymptoms.html

Chahine, M., Barnet, C., Olsen, E.T., Chen, L. and Maddy, E. (2005). On the determinationof atmospheric minor gases by the method of vanishing partial derivatives with application to CO_2. *Geophys. Res. Lett.* 32: L22803. https://doi.org/10.1029/2005GL024165

Filonchyk, M. and Hurynovich, V. (2020a). Validation of MODIS aerosol products with AERONET measurements of different land cover types in areas over eastern Europe and China. *J. Geovis. Spatial Anal.* 4: 10 https://doi.org/10.1007/s41651-020-00052-9

Filonchyk, M. and Hurynovich, V. (2020b). Spatial distribution and temporal variation of atmospheric pollution in the South Gobi Desert, China, during 2016–2019. *Environ. Sci. Pollut. Res.* https://doi.org/10.1007/s11356-020-09000-y

Griffiths, J. and Woodyatt, A. (2020, January 27). *China goes into emergency mode as number of confirmed Wuhan coronavirus cases reaches 2,700*. CNN. https://www.cnn.com/2020/01/26/asia/wuhan-coronavirus-update-intl-hnk/index.html

Holshue, M.L., DeBolt, C., Lindquist, S., Lofy, K.H., Wiesman, J., Bruce, H. and Diaz, G. (2020). First case of 2019 novel coronavirus in the United States. *N. Engl. J. Med.* 382: 929–936. https://doi.org/10.1056/NEJMoa2001191

Hu, Z., Tang, X., Zheng, C., Guan, M. and Shen, J. (2018). Spatial and temporal analyses of air pollutants and meteorological driving forces in Beijing–Tianjin–Hebei region, China. *Environ. Earth Sci.* 77: 540. https://doi.org/10.1007/s12665-018-7705-y

Huang, Y., Yan, Q. and Zhang, C. (2018). Spatial–temporal distribution characteristics of $PM_{2.5}$ in China in 2016. *J. Geovis. Spatial Anal.* 2: 12. https://doi.org/10.1007/s41651-018-0019-5

Hui, D.S., Azhar, E.I. and Madani, T.A. (2020). The continuing 2019-nCoV epidemic threat of novel coronaviruses to global health — The latest 2019 novel coronavirus outbreak in Wuhan, China. *Int. J. Infect. Dis.* 91: 264–266. https://doi.org/10.1016/j.ijid.2020.01.009

Jribi, S., Ben Ismail, H., Doggui, D. and Debbabi, H. (2020). COVID-19 virus outbreak lockdown: What impacts on household food wastage? *Environ. Dev. Sustain.* 22: 3939–3955. https://dx.doi.org/10.1007%2Fs10668-020-00740-y

Kang, H., Zhu, B., Zhu, C., de Leeuw, G., Hou, X. and Gao, J. (2019). Natural and anthropogenic contributions to long-term variations of SO_2, NO_2, CO, and AOD over East China. *Atmos. Res.* 215: 284–293. https://doi.org/10.1016/j.atmosres.2018.09.012

Kerimray, A., Baimatova, N., Ibragimova, O. P., Bukenov, B., Kenessov, B., Plotitsyn, P. and Karaca, F. (2020). Assessing air quality changes in large cities during COVID-19 lockdowns: The impacts of traffic-free urban conditions in Almaty, Kazakhstan. *Sci. Total Environ.* 730: 139179. https://doi.org/10.1016/j.scitotenv.2020.139179

Kim, S.W., Yoon, S.C., Kim, J. and Kim, S.Y. (2007). Seasonal and monthly variations of columnar aerosol optical properties over East Asia determined from multi-year MODIS, LIDAR, and AERONET Sun/sky radiometer measurements. *Atmos. Environ.* 41: 1634–1651. https://doi.org/10.1016/j.atmosenv.2006.10.044

Krotkov, N.A., Carn, S.A., Krueger, A.J., Bhartia, P.K. and Yang, K. (2006). Band residual difference algorithm for retrieval of SO/sub 2/from the aura ozone monitoring instrument (OMI). *IEEE Trans. Geosci. Remote Sens.* 44: 1259–1266. https://doi.org/10.1109/TGRS.2005.861932

Krotkov, N.A., McLinden, C.A., Li, C., Lamsal, L.N., Celarier, E.A., Marchenko, S.V. and Boersma, K.F. (2015). Aura OMI observations of regional SO_2 and NO_2 pollution changes from 2005 to 2014. *Atmos. Chem. Phys.* 16: 4605–4629. https://doi.org/10.5194/acp-16-4605-2016

Lai, Y. and Brimblecombe, P. (2017). Regulatory effects on particulate pollution in the early hours of Chinese New Year, 2015. *Environ. Monit. Assess.* 189: 467. https://doi.org/10.1007/s10661-017-6167-0

Levelt, P.F., van den Oord, G.H., Dobber, M.R., Malkki, A., Visser, H., de Vries, J. and Saari, H. (2006). The ozone monitoring instrument. *IEEE Trans. Geosci. Remote Sens.* 44: 1093–1101. https://doi.org/10.1109/TGRS.2006.872333

Levy, R.C., Mattoo, S., Munchak, L.A., Remer, L.A., Sayer, A.M., Patadia, F. and Hsu, N.C. (2013). The Collection 6 MODIS aerosol products over land and ocean. *Atmos. Meas. Tech.* 6: 2989. https://doi.org/10.5194/amt-6-2989-2013

Liu, C., Beierle, S., Butler, T., Liu, J., Hoor, P., Jöckel, P. and Lelieveld, J. (2011). Application of SCIAMACHY and MOPITT CO total column measurements to evaluate model results over biomass burning regions and Eastern China. *Atmos. Chem. Phys.* 11: 6083–6114. https://doi.org/10.5194/acp-11-6083-2011

Muhammad, S., Long, X. and Salman, M. (2020). COVID-19 pandemic and environmental pollution: A blessing in disguise? *Sci. Total Environ.* 727: 138820. https://doi.org/10.1016/j.scitotenv.2020.138820

Myllyvirta, L. (2020, February 19). *Analysis: Coronavirus temporarily reduced China's CO_2 emissions by a quarter*. Carbon Brief. https://www.carbonbrief.org/analysis-coronavirus-has-temporarily-reduced-chinas-co2-emissions-by-a-quarter

Nakada, L.Y.K. and Urban, R.C. (2020). COVID-19 pandemic: Impacts on the air quality during the partial lockdown in São Paulo state, Brazil. *Sci. Total Environ.* 730: 139087. https://doi.org/10.1016/j.scitotenv.2020.139087

Pagano, T.S., Aumann, H.H., Hagan, D.E. and Overoye, K. (2003). Prelaunch and in-flight radiometric calibration of the atmospheric infrared sounder (AIRS). *IEEE Trans. Geosci. Remote Sens.* 41: 265–273. https://doi.org/10.1109/TGRS.2002.808324

Pagano, T.S., Chahine, M.T. and Olsen, E.T. (2011). Seven years of observations of mid-tropospheric CO_2 from the Atmospheric Infrared Sounder. *Acta Astronaut.* 69: 355–359. https://doi.org/10.1016/j.actaastro.2011.05.016

Perlman, S. (2020). Another decade, another coronavirus. *N. Engl. J. Med.* 382: 760–762. https://doi.org/10.1056/NEJMe2001126

Renuka, K., Gadhavi, H., Jayaraman, A., Rao, S.V. and Lal, S. (2020). Study of mixing ratios of SO_2 in a tropical rural environment in south India. *J. Earth Syst. Sci.* 129: 104. https://doi.org/10.1007/s12040-020-1366-4

Safarian, S., Unnthorsson, R. and Richter, C. (2020). Effect of coronavirus disease 2019 on CO_2 emission in the world. *Aerosol Air Qual. Res.* 20: 1197–1203. https://doi.org/10.4209/aaqr.2020.0.0151

Sayer, A.M., Hsu, N.C., Bettenhausen, C. and Jeong, M.J. (2013). Validation and uncertainty estimates for MODIS Collection 6 "Deep Blue" aerosol data. *J. Geophys. Res.* 118: 7864–7872. https://doi.org/10.1002/jgrd.50600

Wang, Q. and Su, M. (2020). A preliminary assessment of the impact of COVID-19 on environment–A case study of China. *Sci. Total Environ.* 728: 138915. https://doi.org/10.1016/j.scitotenv.2020.138915

Warner, J., Comer, M.M., Barnet, C.D., McMillan, W.W., Wolf, W., Maddy, E. and Sachse, G. (2007). A comparison of satellite tropospheric carbon monoxide measurements from AIRS and MOPITT during INTEX-A. *J. Geophys. Res.* 112: D12S17. https://doi.org/10.1029/2006JD007925

World Health Organization (WHO) (2020a). Naming the coronavirus disease (COVID-19) and the virus that causes it. https://www.who.int/emergencies/diseases/novel-coronavirus-2019/technical-guidance/naming-the-coronavirus-disease-(covid-2019)-and-the-virus-that-causes-it

World Health Organization (WHO) (2020b). WHO coronavirus disease (COVID-19) dashboard. https://covid19.who.int

Wu, Y., Jing, W., Liu, J., Ma, Q., Yuan, J., Wang, Y. and

Liu, M. (2020). Effects of temperature and humidity on the daily new cases and new deaths of COVID-19 in 166 countries. *Sci. Total Environ.* 729: 139051. https://doi.org/10.1016/j.scitotenv.2020.139051

Xiong, X., Barnet, C., Maddy, E., Sweeney, C., Liu, X. and Zhou, L. (2008). Characterization and validation of methane products from the atmospheric infrared sounder (AIRS). *J. Geophys. Res.* 113: G00A01. https://doi.org/10.1029/2007JG000500

Xu, K., Cui, K., Young, L.H., Wang, Y.F., Hsieh, Y.K., Wan, S. and Zhang, J. (2020b). Air quality index, indicatory air pollutants and impact of COVID-19 event on the air quality near central China. *Aerosol Air Qual. Res.* 20: 1204–1221. https://doi.org/10.4209/aaqr.2020.04.0139

Xu, K.J., Cui, K.P., Young, L.H., Hsieh, Y.K., Wang, Y.F., Zhang, J.J. and Wan, S. (2020a). Impact of the COVID-19 event on air quality in central China. *Aerosol Air Qual. Res.* 20: 915–929. https://doi.org/10.4209/aaqr.2020.04.0150

Yan, H., Chen, L., Tao, J., Su, L., Huang, J., Han, D. and Yu, C. (2012). Corrections for OMI SO_2 BRD retrievals influenced by row anomalies. *Atmos. Meas. Tech.* 5: 2635–2646. https://doi.org/10.5194/amt-5-2635-2012

Zhang, L., Jiang, H., Lu, X. and Jin, J. (2016). Comparison analysis of global carbon monoxide concentration derived from SCIAMACHY, AIRS, and MOPITT. *Int. J. Remote Sens.* 37: 5155–5175. https://doi.org/10.1080/01431161.2016.1230282

Zhang, Y., He, C.Q., Tang, B.J. and Wei, Y.M. (2015). China's energy consumption in the building sector: A life cycle approach. *Energy Build.* 94: 240–251. https://doi.org/10.1016/j.enbuild.2015.03.011

Zhang, Y., Wei, J., Tang, A., Zheng, A., Shao, Z. and Liu, X. (2017). Chemical characteristics of $PM_{2.5}$ during 2015 spring festival in Beijing, China. *Aerosol Air Qual. Res.* 17: 1169–1180. https://doi.org/10.4209/aaqr.2016.08.0338

Zhao, T. (2020). The economy was affected by the impact of the epidemic in the first quarter, and the long-term development trend has not changed. http://www.stats.gov.cn/tjsj/zxfb/202004/t20200419_1739666.html

Zhu, Y.J., Xie, J.G., Huang, F.M. and Cao, L.Q. (2020). Association between short-term exposure to air pollution and COVID-19infection: Evidence from China. *Sci. Total Environ.* 727: 138704. https://doi.org/10.1016/j.scitotenv.2020.138704

Received for review, May 15, 2020
Revised, June 6, 2020
Accepted, June 7, 2020